ESI for:

Controlling phase in low-nuclearity calixarene-capped porous coordination cages with ligand functionalization

Michael R. Dworzak,‡ Casey A. Rowland,‡ Glenn P. A. Yap, and Eric D. Bloch*
Department of Chemistry and Biochemistry, University of Delaware, Newark, Delaware 19716, United States

List of Contents

Detailed Synthetic Procedures

Synthesis of 2,7-dibromo-3,6-diacetyl-9-phenyl-carbazole: 2,7-dibromo-9-phenyl-carbazole (10 g, 24.9 mmol) was dissolved in 100 mL DCM. In a separate RBF $AlCl_3$ (9.96 g, 74.7 mmol) and Acetyl Chloride (8.85 mL, 124.5 mmol) were suspended in 100 mL DCM. To this suspension the 2,7-dibromo-9-phenyl-carbazole solution was added dropwise. The reaction mixture was set to stir at RT for 12 h. The reaction mixture was then poured into 300 mL of DI H2O and precipitated solids were collected via vacuum filtration. (Yield: g, %) 1H NMR (400 MHz, DMSO-d6) δ = 8.91 (s, 2H), 7.69 (m, 5H), 7.53 (s, 2H), 2.72 (s, 6H).

Synthesis of 2,7-dibromo-9-phenyl-carbazole dicarboxylic acid: 2,7-dibromo-3,6-diacetyl-9-phenyl-carbazole (10.5 g, 21.7 mmol) was dissolved in 250 mL 1,4-Dioxane. In a separate RBF NaOH (56.4 g, 1.41 mol) was dissolved in 250 mL DI H2O. The NaOH (aq) solution was cooled to 0 °C in an ice bath and set to stir at 0 °C for 0.5 h. To the cooled NaOH (aq) solution 25 mL Br2 was added dropwise. The prepared NaOBr (aq) solution continued to stir at 0 °C for an additional 0.5 h. The NaOBr (aq) solution was added dropwise to the 2,7-dibromo-3,6-diacetyl-9-phenyl-carbazole solution. After complete addition the reaction mixture was set to heat at 100 °C for 12 h. After cooling to RT the reaction mixture was poured into 600 mL of saturated Na2SO3 (aq) solution. The reaction mixture was then acidified to pH = 1 and precipitated solids were collected via vacuum filtration. (Yield: g, %) 1H NMR (400 MHz, DMSO-d6) δ = 8.92 (s, 2H), 7.70 (m, 5H), 7.51 (s, 2H).

Synthesis of dimethyl 2,7-dibromo-9-phenyl-carbazole-3,6-dicarboxylate: 2,7-dibromo-9-phenyl-cdc (12.4 g, 24.9 mmol) and K2CO3 (17.2 g, 124.5 mmol) were suspended in 250 mL DMF. The reaction mixture was set to stir at RT for 0.5 h. To the stirring suspension Iodomethane (4.7 mL, 74.7 mmol) were added and the reaction mixture set to heat at 100 °C for 12 h. After cooling to RT the reaction mixture was poured into 500 mL of DI H2O and precipitated solids were collected via vacuum filtration. (Yield: g, %) 1H NMR (400 MHz, DMSO-d6) δ = 8.92 (s, 2H), 7.71 (m, 5H), 7.55 (s, 2H), 3.91 (s, 6H).

Synthesis of dimethyl 2,7,9-triphenyl-carbazole-3,6-dicarboxylate: Dimethyl 2,7-dibromo-9-phenyl-carbazole-3,6-dicarboxylate (10.2 g, 19.8 mmol), phenylboronic acid (12.07 g, 99 mmol) and K2CO3 (21.9 g, 158.4 mmol) were suspended in 300 mL of 1,4-Dioxane. The reaction mixture was sparged with N2 for 0.5 h. Pd(PPh3)4 (500 mg, 2 mol%) was added and the reaction mixture was set to heat under N2 at 100 °C for 48 h. After cooling to RT the reaction mixture was poured into 1 L DI H2O and precipitated solids were collected via vacuum filtration. (Yield: g, %) 1H NMR (400 MHz, DMSO-d6) δ = 8.93 (s, 2H), 7.74 – 7.56 (d,t,t, 5H), 7.45 – 7.30 (m, 10H), 7.24 (s, 2H) 3.65 (s, 6H).

2,7,9-triphenyl-carbazole dicarboxylic acid: Dimethyl 2,7,9-triphenyl-carbazole-3,6-dicarboxylate (9.6 g, 18.8 mmol) was suspended in a solvent mixture containing 100 mL MeOH, 100 mL THF and 150 mL 2 M KOH (aq) solution. The reaction mixture was set to reflux for 12 h. After cooling to RT the reaction mixture was filtered, the filtrate was acidified to pH = 1 and precipitated solids were collected via vacuum filtration. (Yield: g, %) 1H NMR (400 MHz, DMSO-d6) δ = 12.64 (s, 2H), 8.88 (s, 2H), 7.77 – 7.5 (m, 5H), 7.53 (s, 2H), 7.43 – 7.30 (m, 10H), 7.20 (s, 2H).

Synthesis of Mg-TriPhen-cdc: MgCl2 · 6 H2O (101.7 mg, 0.5 mmol) and PTBSC4A (84.9 mg, 0.1 mmol) were dissolved in 12 mL of a 3:1 DMF/MeOH mixture (9 mL DMF, 3 mL MeOH) in a 20 mL scintillation vial and set to heat at 85 °C for 12 h in an Al block. After cooling to RT 2,7,9-triphenyl-cdc (159.6 mg, 0.33 mmol) was added and the reaction mixture returned to heat at 85 °C for an additional 12 h in an Al block. The reaction vial was removed from heat in the Al block to cool slowly. After cooling to RT diffraction quality crystals were harvested.

Synthesis of Mn-TriPhen-cdc: MnCl2 · 4 H2O (99.0 mg, 0.5 mmol) and PTBSC4A (84.9 mg, 0.1 mmol) were dissolved in 12 mL of a 2:1 DMF/MeOH mixture (8 mL DMF, 4 mL MeOH) in a 20 mL scintillation vial and set to heat at 85 °C for 12 h in an Al block. After cooling to RT 2,7,9-triphenyl-cdc (159.6 mg, 0.33 mmol) was added and the reaction mixture returned to heat at 85 °C for an additional 12 h in an Al block. THe reaction vial was removed from heat in the Al block to cool slowly. After cooling to RT diffraction quality crystals were harvested.

Synthesis of Co-TriPhen-cdc: Co(NO3)2 · 6 H2O (145.5 mg, 0.5 mmol) and PTBSC4A (84.9 mg, 0.1 mmol) were dissolved in 10 mL DMF in a 20 mL scintillation vial and set to heat at 85 °C for 12 h in an Al block. After cooling to RT 2,7,9-triphenyl-cdc (159.6 mg, 0.33 mmol) was added and the reaction mixture returned to heat at 85 °C for an additional 12 h in an Al block. After cooling to RT the reaction mixture was diffused with MeOH to obtain diffraction quality crystals.

Synthesis of Ni-TriPhen-cdc: Ni(NO3)2 · 6 H2O (145.4 mg, 0.5 mmol) and PTBSC4A (84.9 mg, 0.1 mmol) were dissolved in 10 mL DMF in a 20 mL scintillation vial and set to heat at 85 °C for 12 h in an Al block. After cooling to RT 2,7,9-triphenyl-cdc (159.6 mg, 0.33 mmol) was added and the reaction mixture returned to heat at 85 °C for an additional 12 h in an Al block. After cooling to RT the reaction mixture was diffused with EtOH to obtain diffraction quality crystals.

^{1}H NMR Spectra

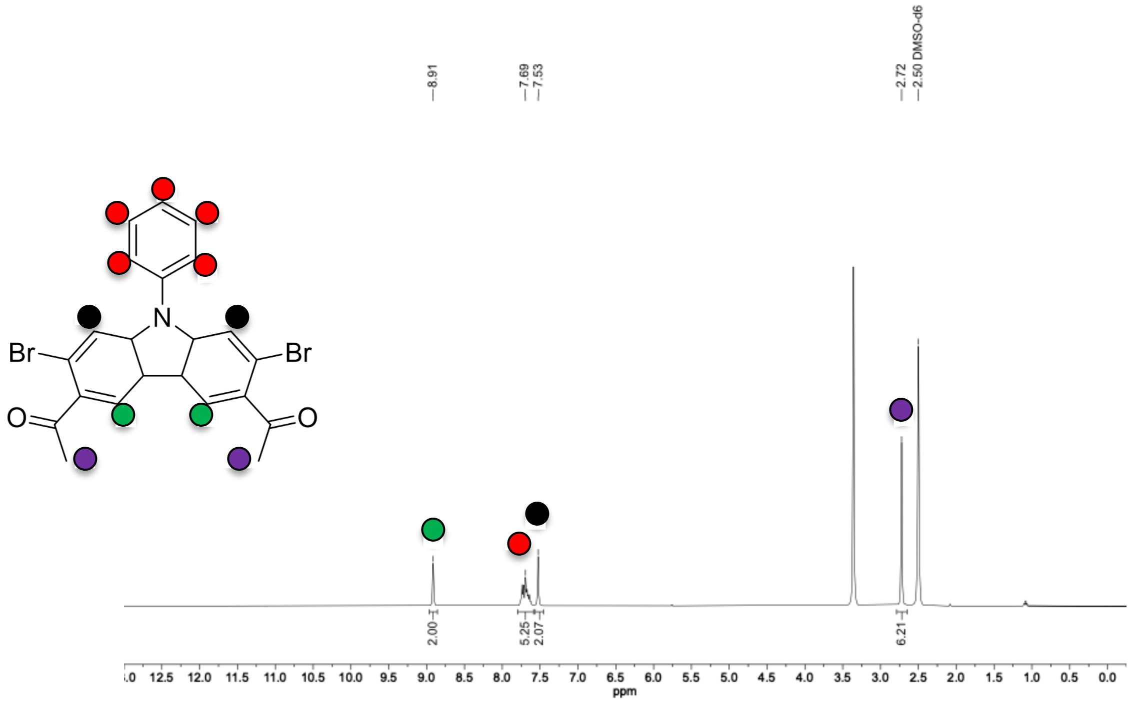

Figure S1. ^{1}H-NMR (400 MHz, DMSO-d_6) spectrum of 2,7-dibromo-3,6-diacetyl-9-phenyl-carbazole.

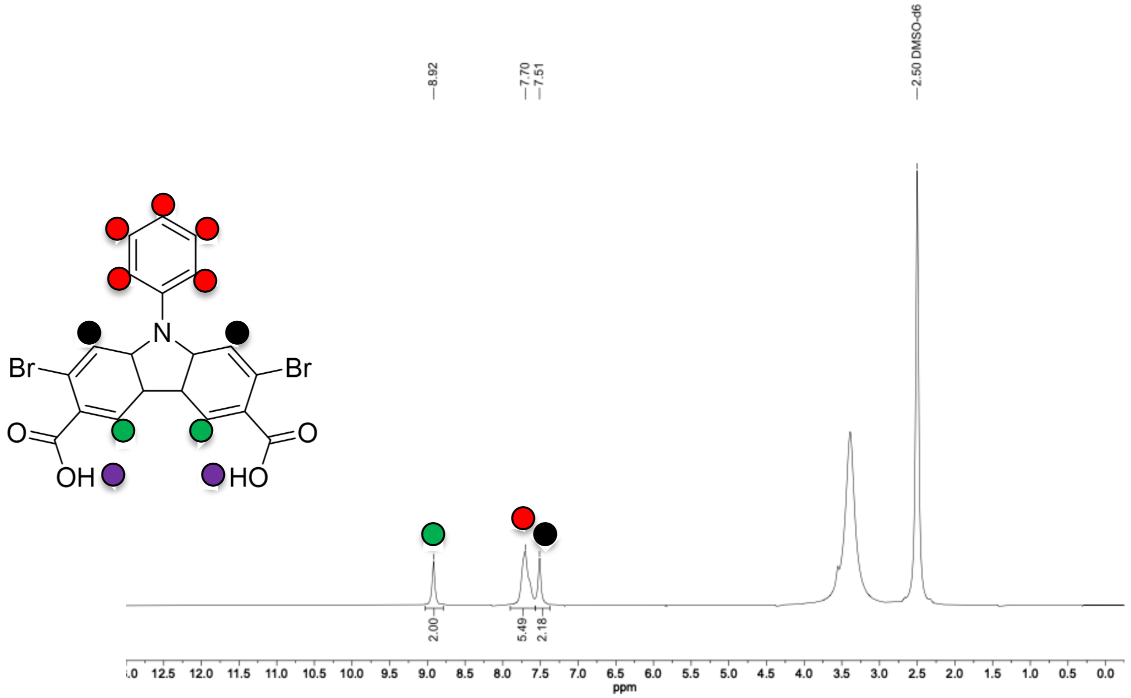

Figure S2. ^{1}H-NMR (400 MHz, DMSO-d_6) spectrum of 2,7-dibromo-9-phenyl-carbazole-dicarboxylic acid.

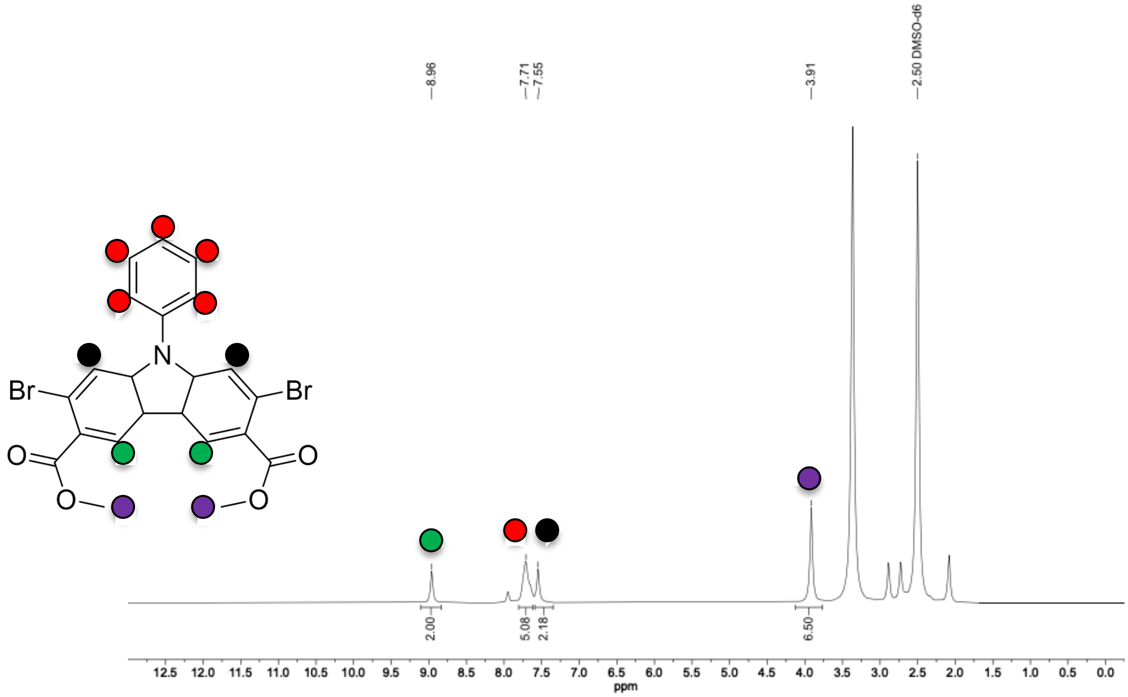

Figure S3. ^{1}H-NMR (400 MHz, DMSO-d_6) spectrum of dimethyl-2,7-dibromo-9-phenyl-carbazole-dicarboxylate.

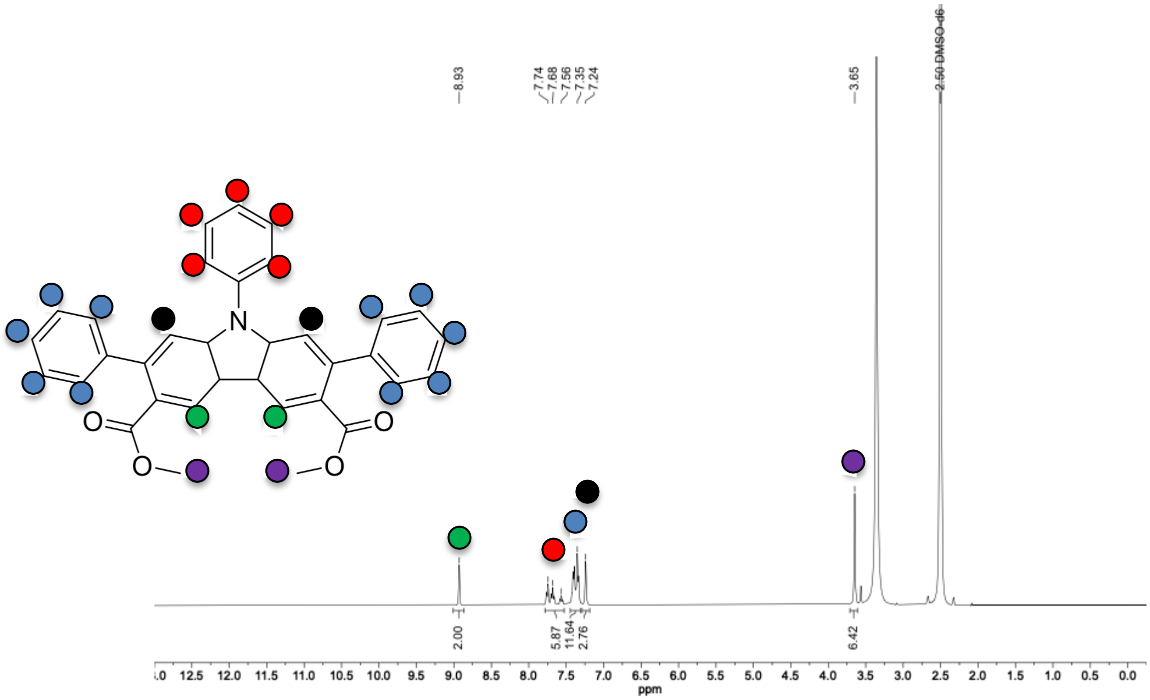

Figure S4. ^{1}H-NMR (400 MHz, DMSO-d_6) spectrum of dimethyl-2,7,9-triphenyl-carbazole dicarboxylate.

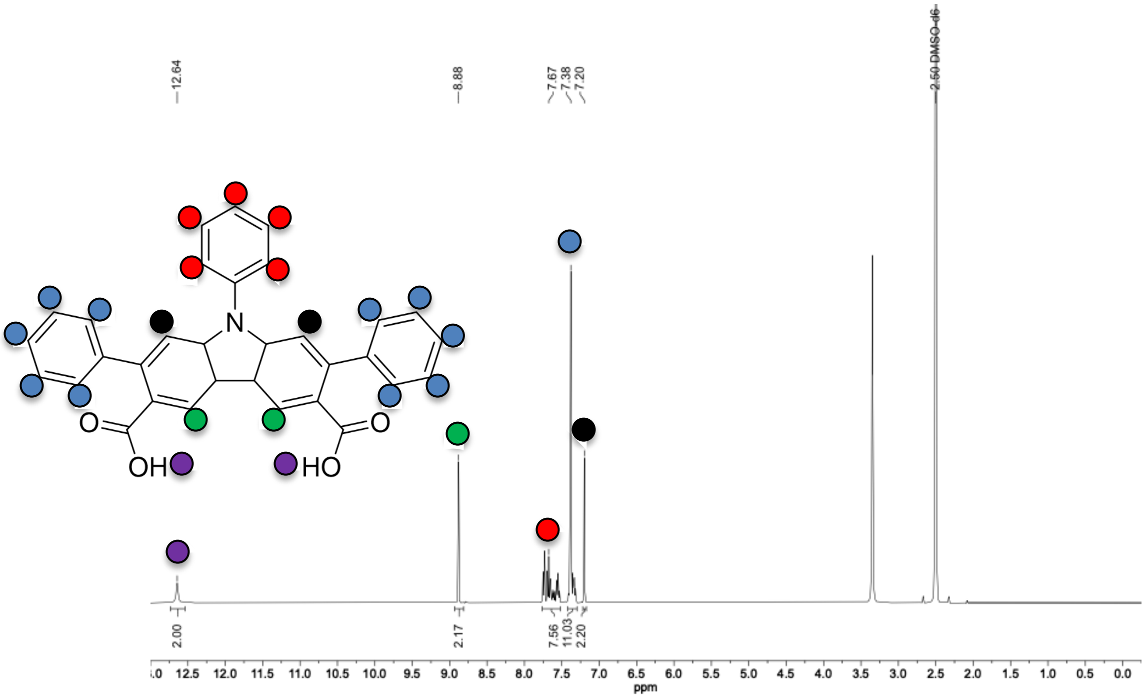

Figure S5. ^{1}H-NMR (400 MHz, DMSO-d_6) spectrum of 2,7,9-triphenyl-carbazole dicarboxylic acid.

IR Spectra

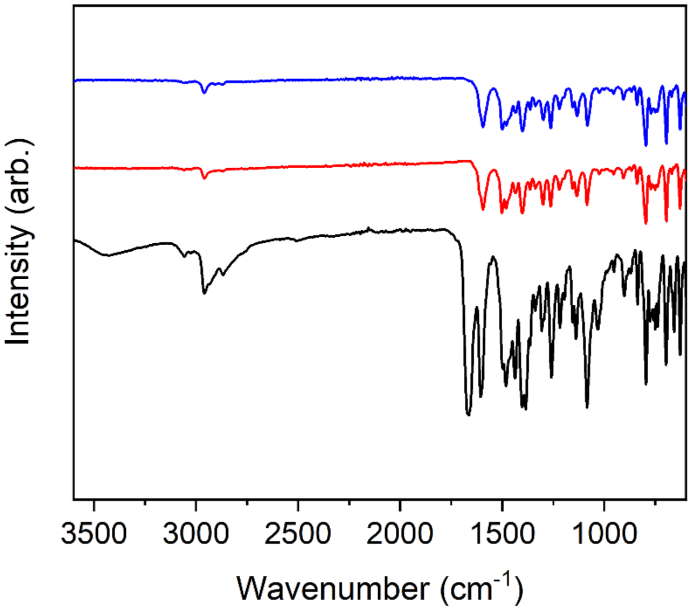

Figure S6. IR spectra of Mg-TriPhen-cdc as synthesized (black), solvent exchanged with MeOH (red), and activated (blue).

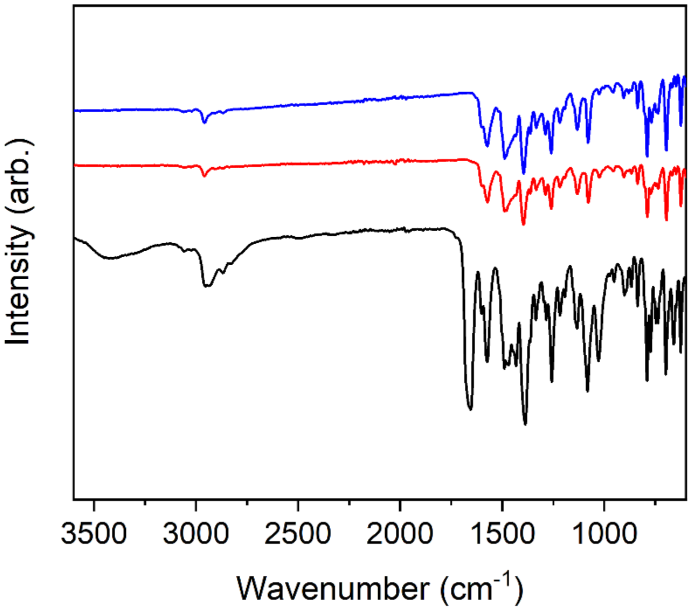

Figure S7. IR spectra of Mn-TriPhen-cdc as synthesized (black), solvent exchanged with MeOH (red), and activated (blue).

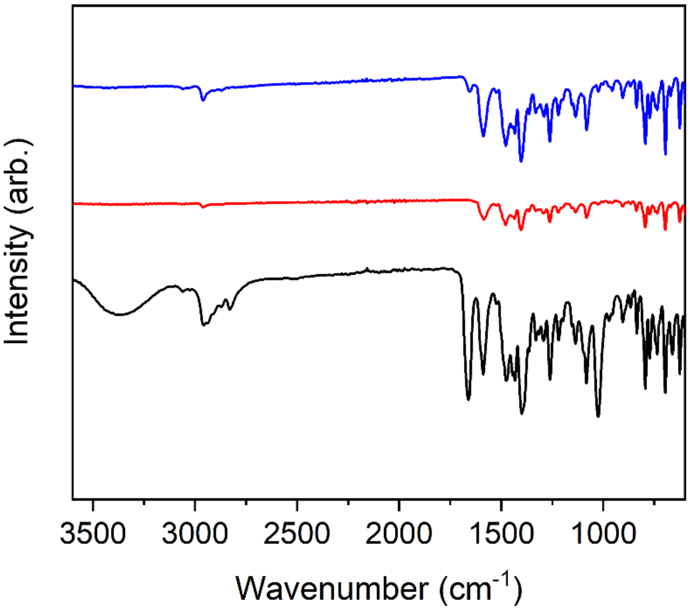

Figure S8. IR spectra of Co-TriPhen-cdc as synthesized (black), solvent exchanged with MeOH (red), and activated (blue).

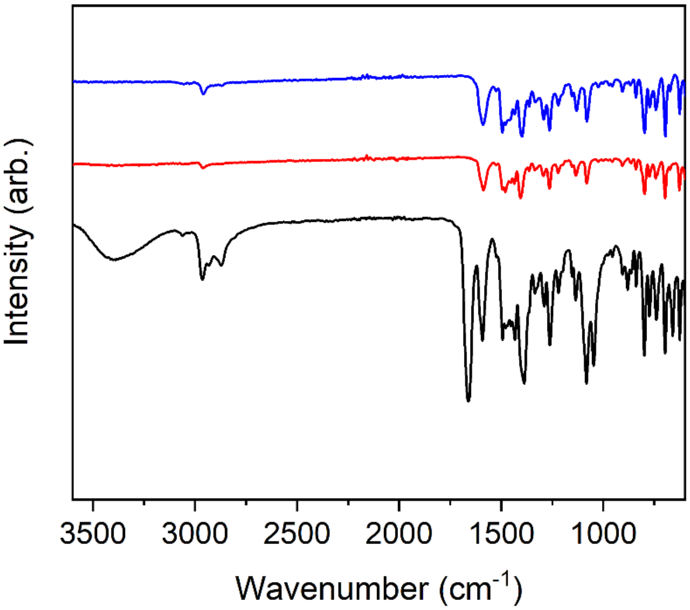

Figure S9. IR spectra of Ni-TriPhen-cdc as synthesized (black), solvent exchanged with MeOH (red), and activated (blue).

Thermogravimetric Analysis (TGA)

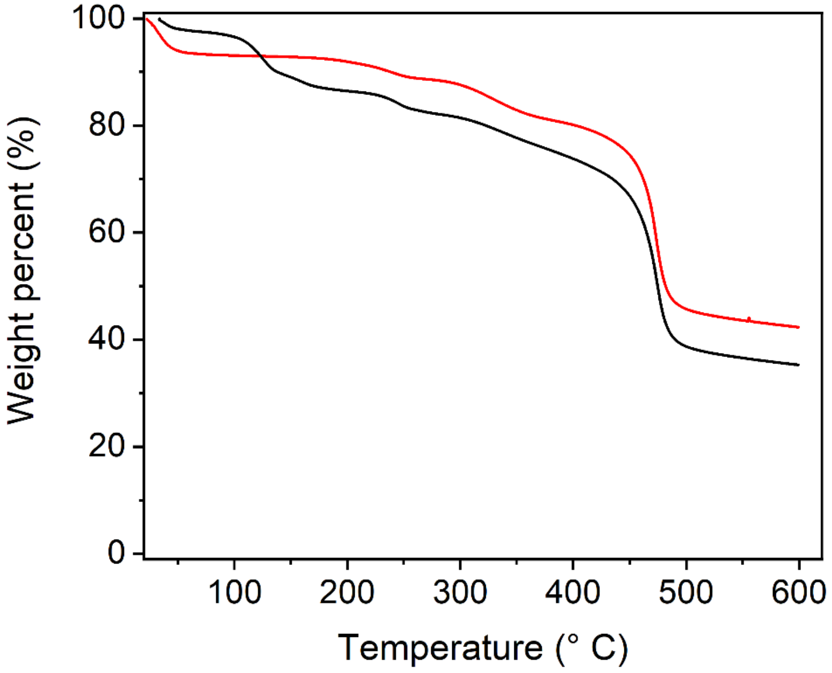

Figure S10. TGA of Mg-TriPhen-cdc as synthesized (black) and solvent exchanged with MeOH (red).

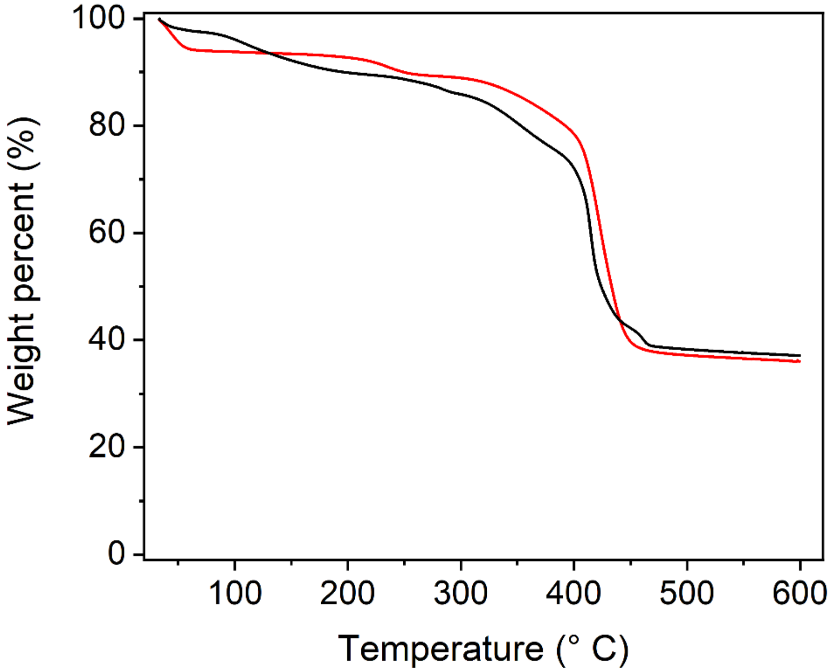

Figure S11. TGA of Mn-TriPhen-cdc as synthesized (black) and solvent exchanged with MeOH (red).

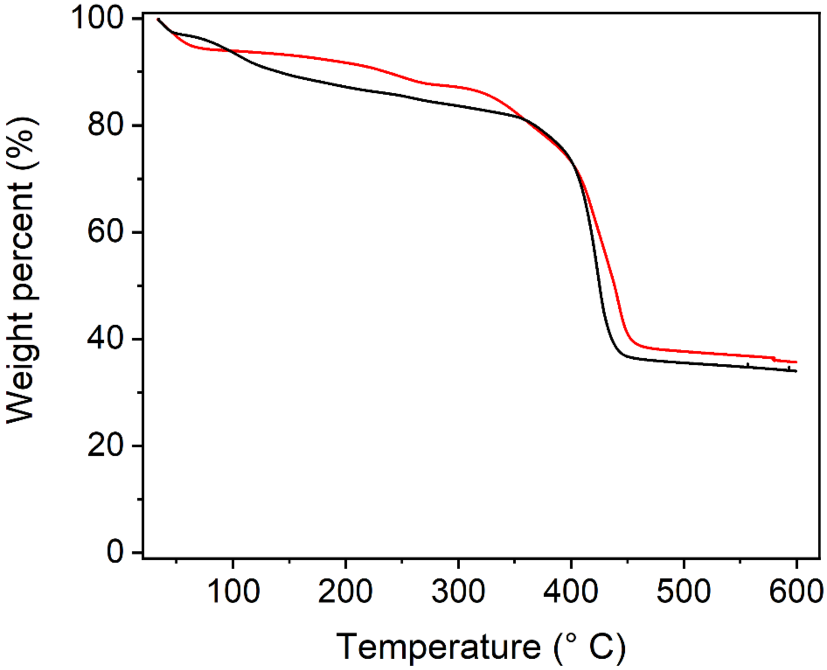

Figure S12. TGA of Co-TriPhen-cdc as synthesized (black) and solvent exchanged with MeOH (red).

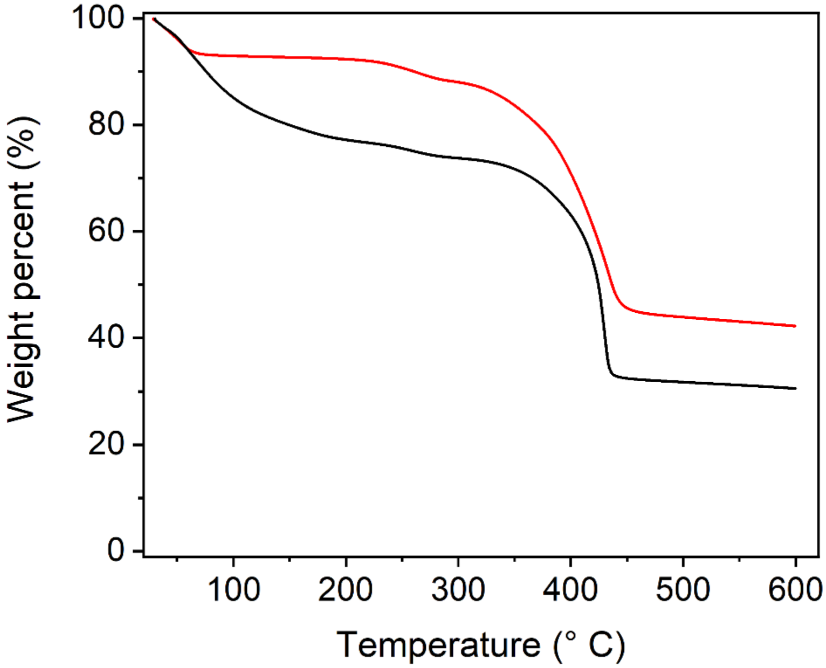

Figure S13. TGA of Ni-TriPhen-cdc as synthesized (black) and solvent exchanged with MeOH (red).

Gas Adsorption Measurements

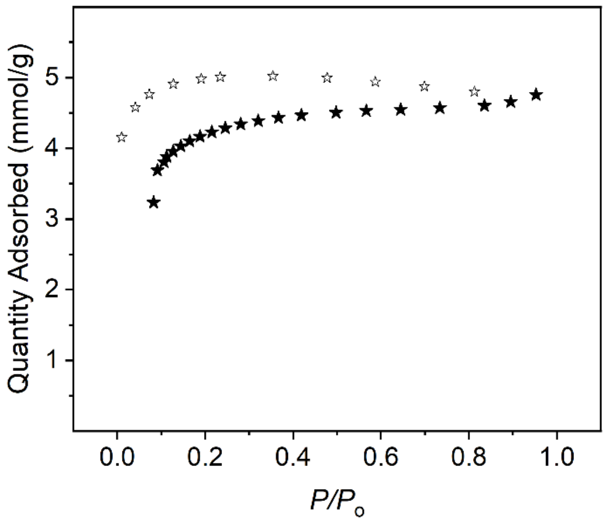

Figure S14. N_2 adsorption (solid black stars) and desorption (hollow black stars) at 77 K for Mg-TriPhenyl-cdc.

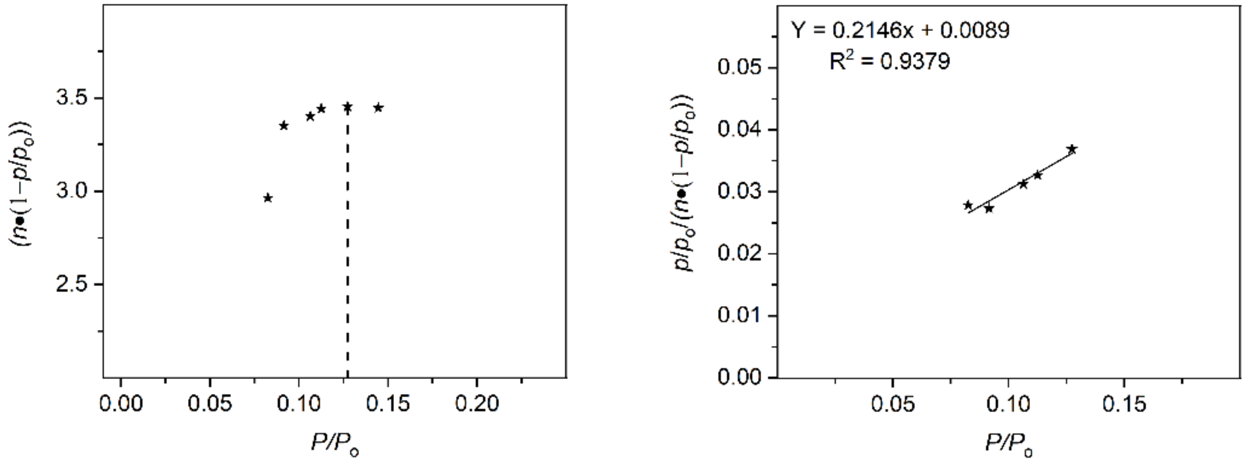

Figure S15. Left: Plot of $n(1\text{-}P/P_0)$ vs. P/P_0 to determine the maximum P/P_0 used in the BET linear fit according to the first BET consistency criterion for N_2 adsorption at 77 K for the Mg-TriPhenyl-cdc. Right: The slope of the best fit line for $P/P_0 < 0.1264$ is 0.2146 and the y-intercept is 0.0089, which satisfies the second BET consistency criterion. This results in a measured surface area of 455 m^2/g to N_2.

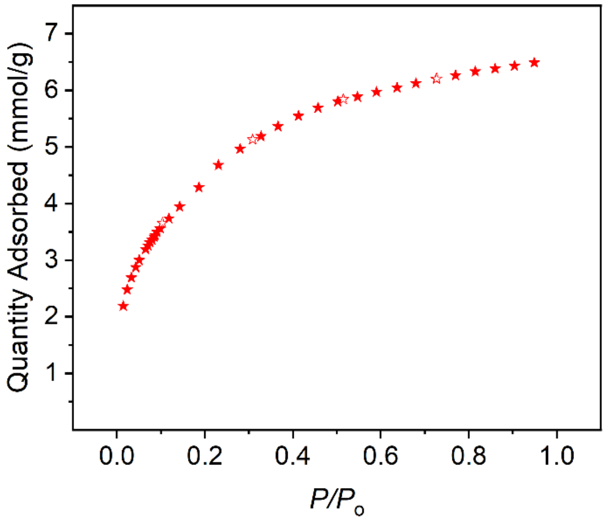

Figure S16. CO_2 adsorption (solid red stars) and desorption (hollow red stars) 195 K for Mg-TriPhenyl-cdc.

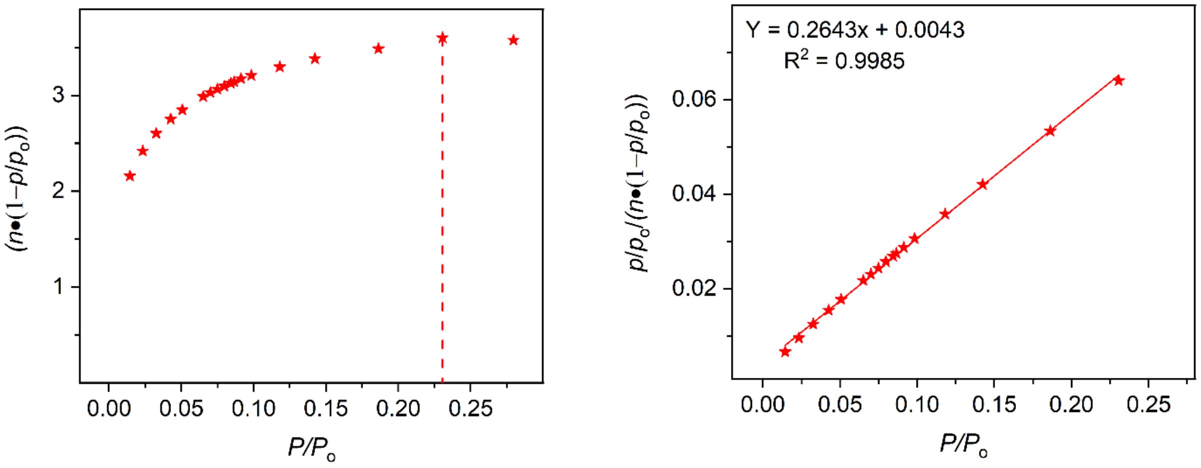

Figure S17. Left: Plot of n(1-P/P_0) vs. P/P_0 to determine the maximum P/P_0 used in the BET linear fit according to the first BET consistency criterion for CO_2 adsorption at 195 K for the Mg-TriPhenyl-cdc. Bottom right: The slope of the best fit line for $P/P_0 < 0.231$ is 0.2643 and the y-intercept is 0.0043, which satisfies the second BET consistency criterion. This results in a measured surface area of 387 m^2/g to CO_2.

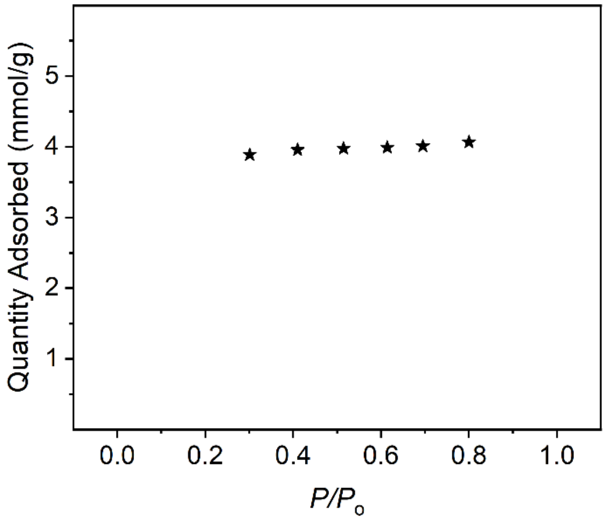

Figure S18. N_2 adsorption (solid black stars) and desorption (hollow black stars) at 77 K for Mn-TriPhenyl-cdc.

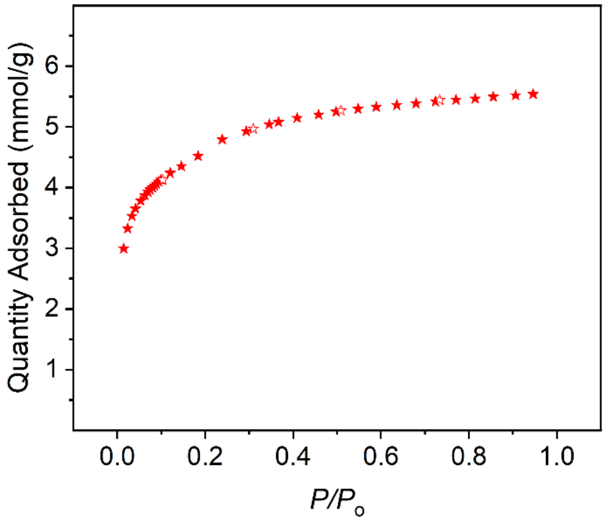

Figure S19. CO_2 adsorption (solid red stars) and desorption (hollow red stars) 195 K for Mn-TriPhenyl-cdc.

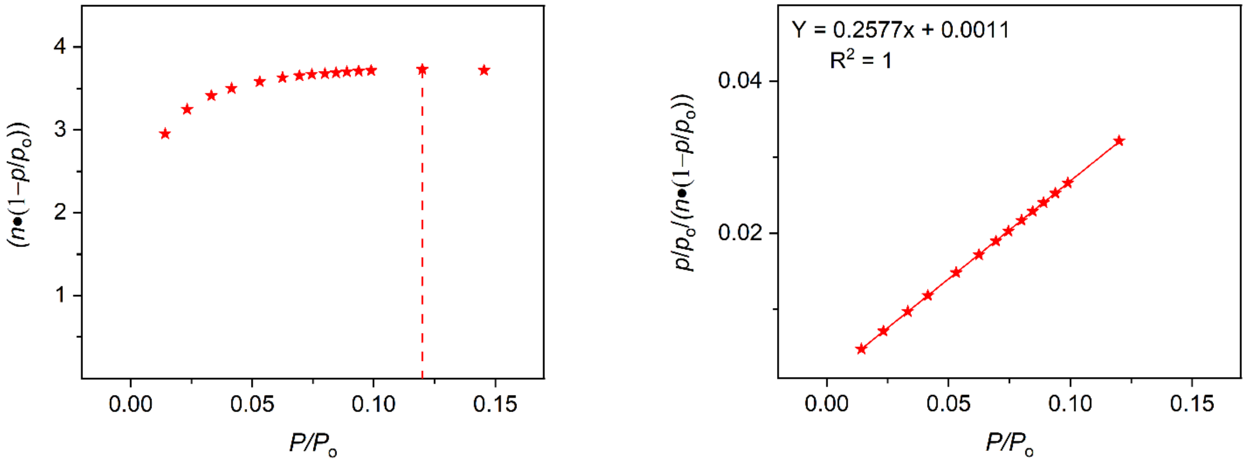

Figure S20. Bottom left: Plot of n(1-P/P$_0$) vs. P/P$_0$ to determine the maximum P/P$_0$ used in the BET linear fit according to the first BET consistency criterion for CO_2 adsorption at 195 K for the Mn-TriPhenyl-cdc. Bottom right: The slope of the best fit line for P/P$_0$ < 0.120 is 0.2577 and the y-intercept is 0.0011, which satisfies the second BET consistency criterion. This results in a measured surface area of 397 m^2/g to CO_2.

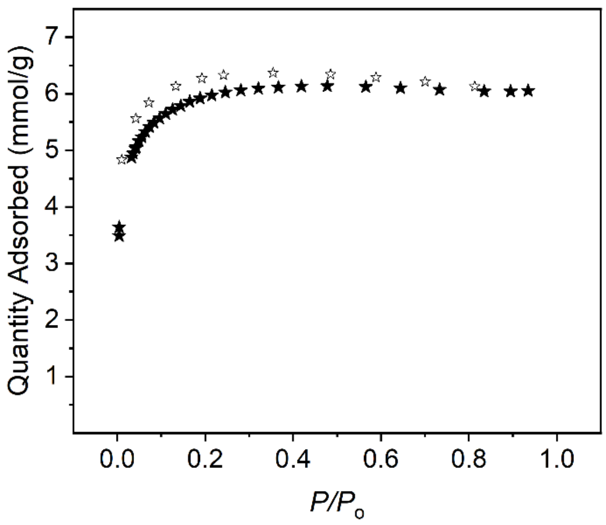

Figure S21. N_2 adsorption (solid black stars) and desorption (hollow black stars) at 77 K for Co-TriPhenyl-cdc.

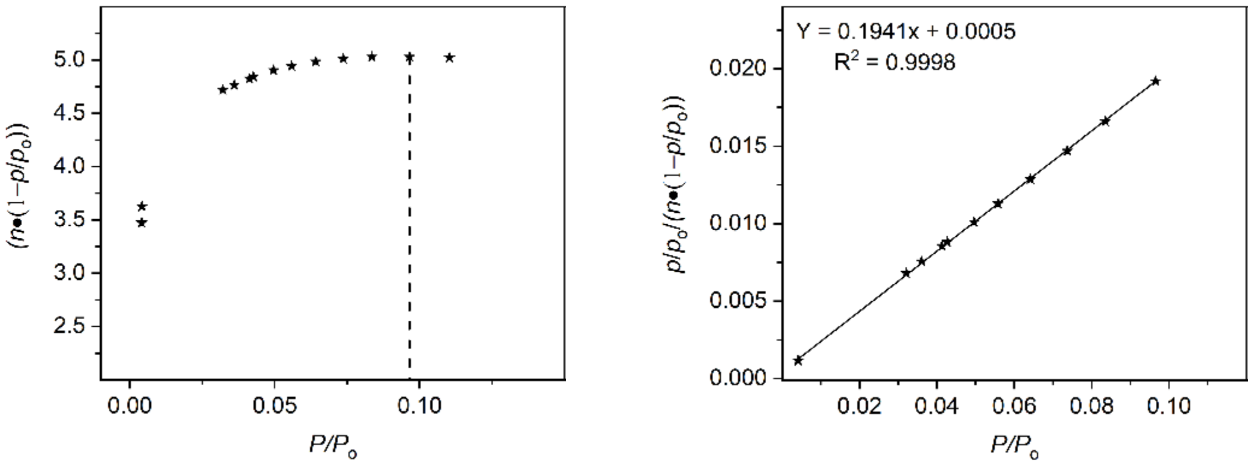

Figure S22. Top left: Plot of $n(1-P/P_0)$ vs. P/P_0 to determine the maximum P/P_0 used in the BET linear fit according to the first BET consistency criterion for N_2 adsorption at 77 K for the Co-TriPhenyl-cdc. Top right: The slope of the best fit line for $P/P_0 < 0.0965$ is 0.1941 and the y-intercept is 0.0005, which satisfies the second BET consistency criterion. This results in a measured surface area of 503 m^2/g to N_2.

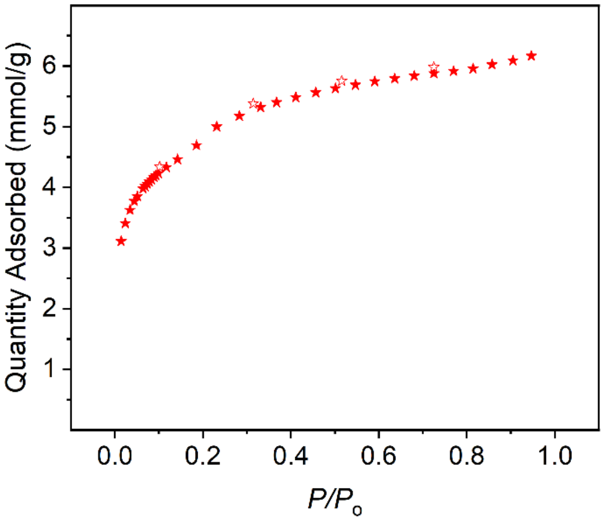

Figure S23. CO$_2$ adsorption (solid red stars) and desorption (hollow red stars) at 195 K for Co-TriPhenyl-cdc.

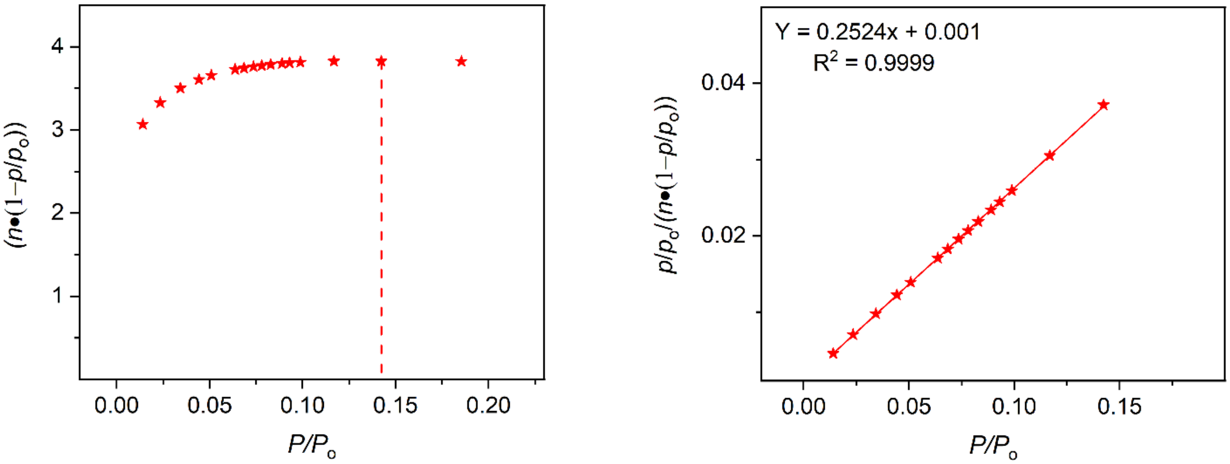

Figure S24. Top left: Plot of n(1-P/P$_0$) vs. P/P$_0$ to determine the maximum P/P$_0$ used in the BET linear fit according to the first BET consistency criterion for N$_2$ adsorption at 77 K for the Co-TriPhenyl-cdc. Top right: The slope of the best fit line for P/P$_0$ < 0.1423 is 0.2524 and the y-intercept is 0.001, which satisfies the second BET consistency criterion. This results in a measured surface area of 406 m^2/g to N$_2$.

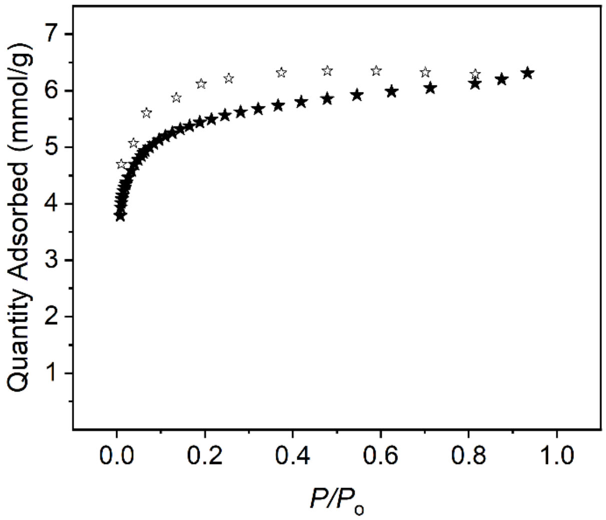

Figure S25. N_2 adsorption (solid black stars) and desorption (hollow black stars) at 77 K for Ni-TriPhenyl-cdc.

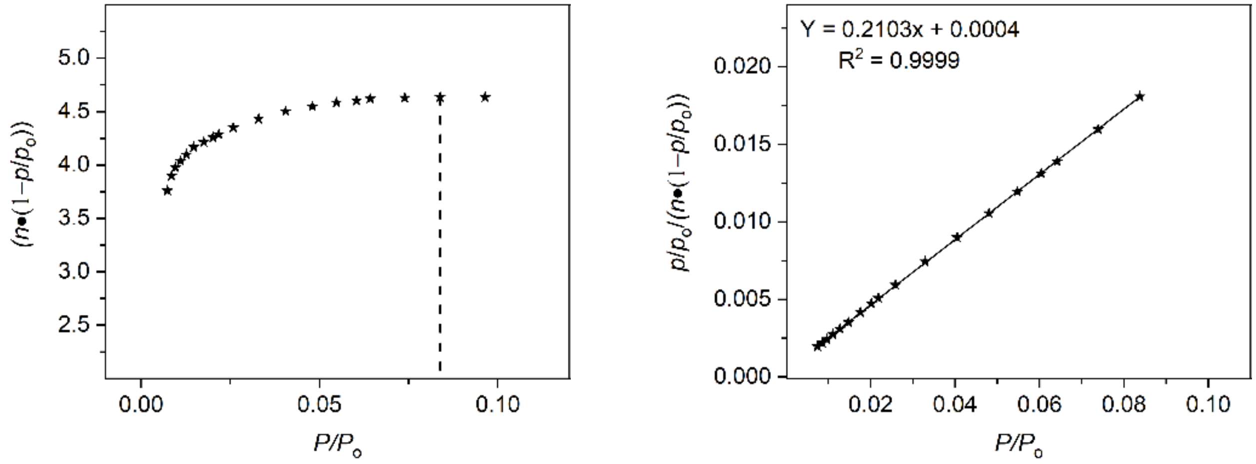

Figure S26. Top left: Plot of $n(1-P/P_0)$ vs. P/P_0 to determine the maximum P/P_0 used in the BET linear fit according to the first BET consistency criterion for N_2 adsorption at 77 K for the Ni-TriPhenyl-cdc. Top right: The slope of the best fit line for $P/P_0 < 0.0838$ is 0.2103 and the y-intercept is 0.0004, which satisfies the second BET consistency criterion. This results in a measured surface area of 464 m^2/g to N_2.

Table S1. Nitrogen and CO2 surface areas of novel calix[4]arene capped cages.

Material	**N_2 BET (m^2/g)**	**N_2 Langmuir (m^2 /g)**	**CO_2 BET (m^2 /g)**	**CO_2 Langmuir (m_2 /g)**
Mg-TriPhenyl-cdc	455	485	387	744
Mn-TriPhenyl-cdc	---	399	397	593
Co-TriPhenyl-cdc	503	596	406	663
Ni-TriPhenyl-cdc	464	619	---	---

Crystal Structures

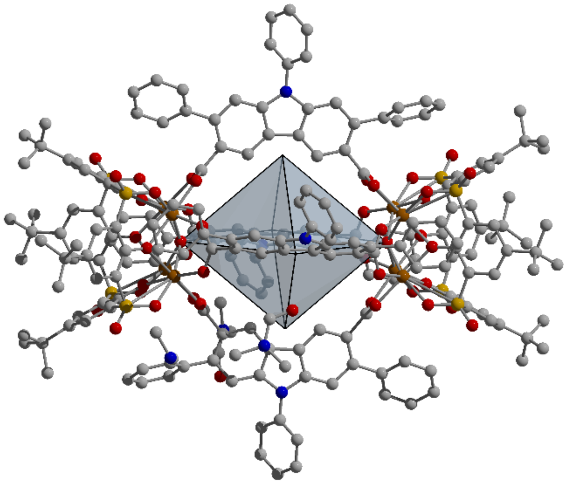

Figure S27. Single crystal structural depiction of the previously reported Mg-TriPhenyl-cdc.

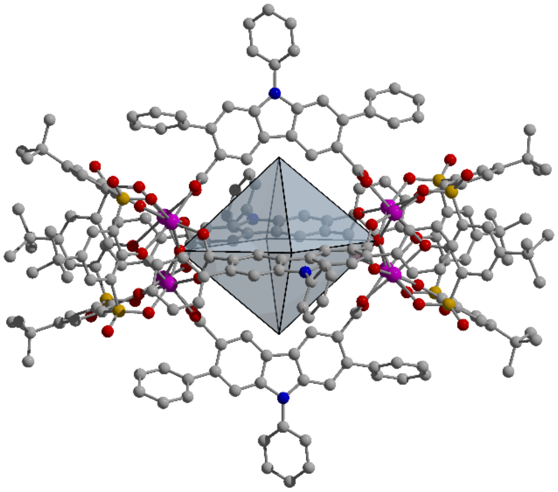

Figure S28. Single crystal structural depiction of the previously reported Mn-TriPhenyl-cdc.

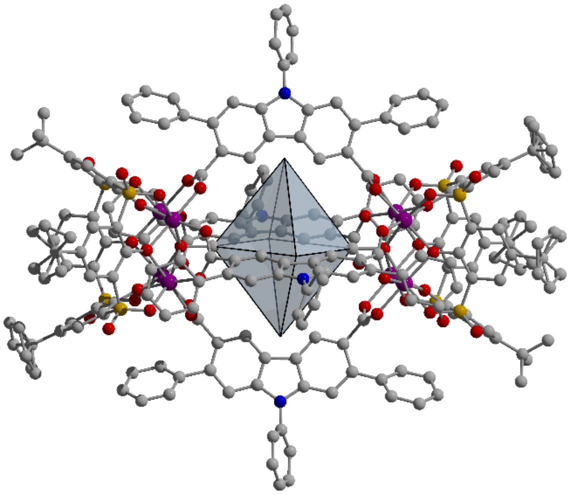

Figure S29. Single crystal structural depiction of the previously reported Co-TriPhenyl-cdc.

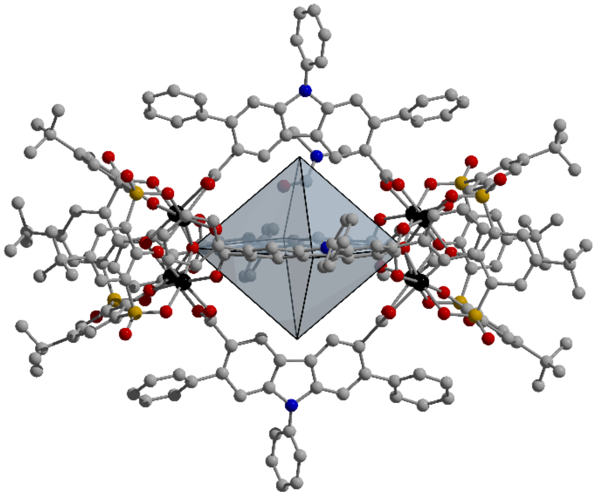

Figure S30. Single crystal structural depiction of the previously reported Ni-TriPhenyl-cdc.

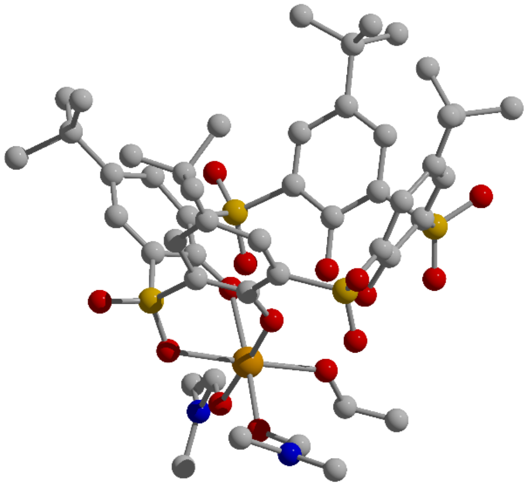

Figure S31. Iron/Sulfonylcalix[4]arene metal cluster.

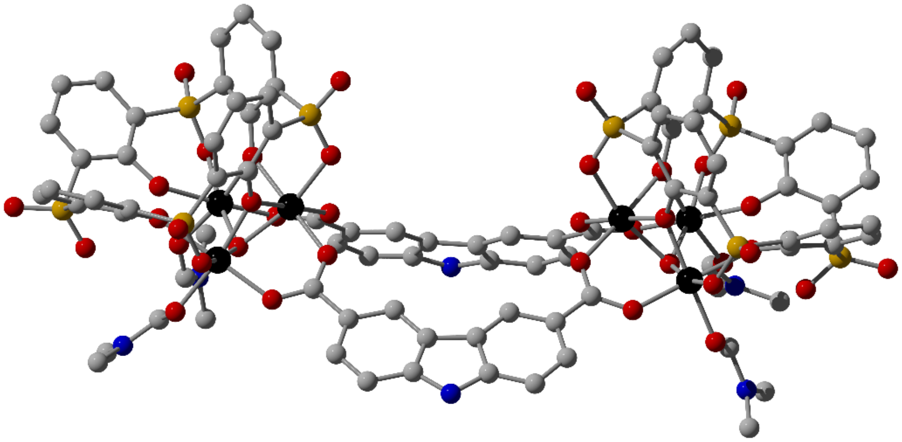

Figure S32. Open Nickel 9H-cdc complex.

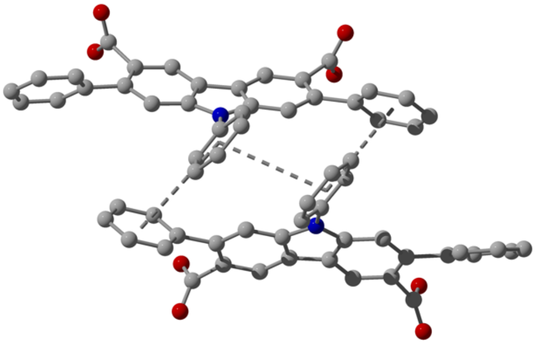

Figure S33. Edge-to-face (T-shaped) pi-pi stacking between Mg-TriPhenyl-cdc cages with distances of 4.9868(2), 4.2409(2), and 4.9439(3) Å (from left to right).

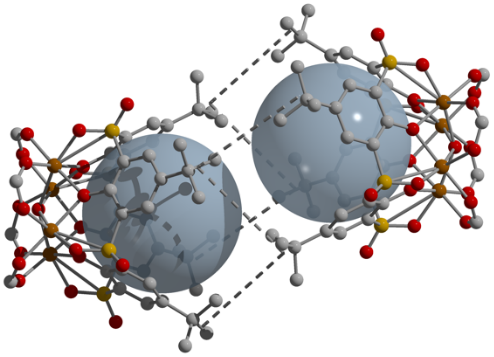

Figure S34. ^{t}Bu- ^{t}Bu interactions between the calixarene units of different Mg-TriPhenyl-cdc cages with distances of 5.5867(3), 5.4049(3), 6.0520(3), 6.0520(3), 5.4049(3) and 5.5867(3) Å from top to bottom.

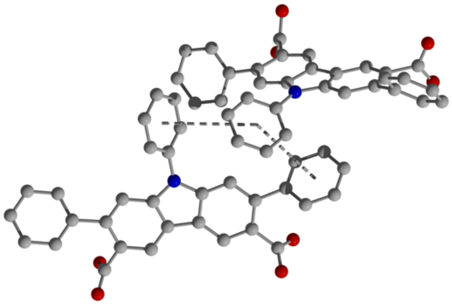

Figure S35. Pseudo edge-to-face (T-shaped) pi-pi stacking between Mn-TriPhenyl-cdc cages with distances of 4.6782 and 4.3545 Å (from left to right).

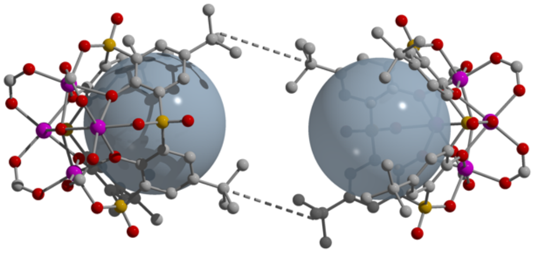

Figure S36. ^{t}Bu- ^{t}Bu interactions between the calixarene units of different Mn-TriPhenyl-cdc cages with distances of 4.7487 and 4.7487 Å from top to bottom.

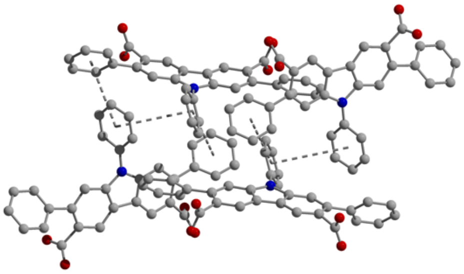

Figure S37. Edge-to-face (T-shaped) pi-pi stacking between Co-TriPhenyl-cdc cages with distances of 4.6245(5), 4.6784(5), 5.4462(5), 5.4462(5), and 4.6784(5) Å (from left to right).

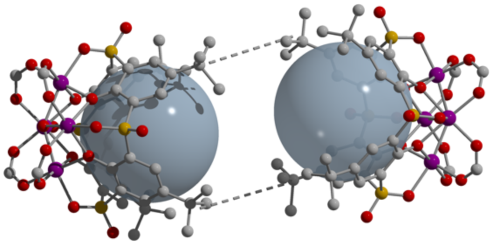

Figure S38. ^{t}Bu-^{t}Bu interactions between the calixarene units of different Co-TriPhenyl-cdc cages with distances of 4.7732(6) and 4.6286(6) Å from top to bottom.

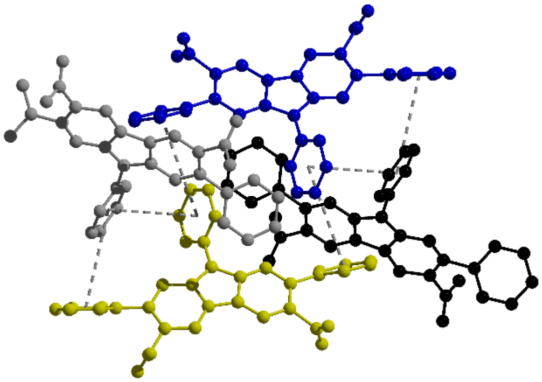

Figure S39. Pseudo edge-to-face (T-shaped) pi-pi stacking between Ni-TriPhenyl-cdc cages with distances of 4.7075(3), 4.6627(3), 5.0057(3), 5.0057(3), 4.6627(3), and 4.7075(3) Å (from left to right).

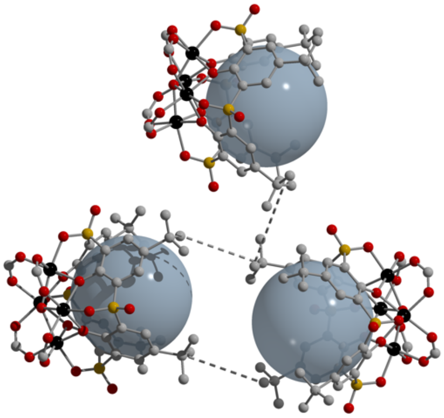

Figure S40. ^{t}Bu-^{t}Bu interactions between the calixarene units of different Ni-TriPhenyl-cdc cages with distances of 5.7182(5), 4.8892(4), and 4.8892(4) Å from top to bottom.

X-ray structural analysis for **(Co-TriPhenyl-cdc)**, **(Ni-9-tButylBenzyl-cdc)**, **(Ni-TriPhenyl-cdc)**, **(Fe-SC4A)**, **(Mg-TriPhenyl-cdc)**, and **(Mn-TriPhenyl-cdc)**: Crystals were mounted using viscous oil, perfluoroalkane or mother liquor onto a plastic mesh and cooled to the data collection temperature. Data were collected on a D8 Venture Photon III diffractometer with Cu-Kα radiation (λ = 1.54178 Å) focused with Goebel mirrors. Unit cell parameters were obtained from fast scan data frames, 1°/s ω, of an Ewald hemisphere. The unit-cell dimensions, equivalent reflections and systematic absences in the diffraction data are consistent with *Cc* and *C*2/*c* for **(Ni-9-tButylBenzyl-cdc)**, and, uniquely, $P2_1/c$ for **(Co-TriPhenyl-cdc)**, **(Ni-TriPhenyl-cdc)eric506**, **(Fe-SC4A)**, and **(Mn-TriPhenyl-cdc)**. No symmetry higher than triclinic was observed in **(Mg-TriPhenyl-cdc)**. Refinement in the centrosymmetric space group option, *C*2/*c*, for the non-unique case, **(Ni-9-tButylBenzyl-cdc)**, yielded chemically reasonable and computationally stable results of refinement. The data were treated with multi-scan absorption corrections.[1] Structures were solved using intrinsic phasing methods[2] and refined with full-matrix, least-squares procedures on F^2.[3] These compounds apparently consistently deposited as weakly diffracting crystals an the data represent the best of several trials.

For **(Co-TriPhenyl-cdc) (Ni-TriPhenyl-cdc)**, **(Mg-TriPhenyl-cdc)**, and **(Mn-TriPhenyl-cdc),** the structure is located at an inversion center. In each structure, presumably disordered solvent molecules were treated as diffused contributions with identities assigned based on the electron counts from the Squeeze results.[4]

Non-hydrogen atoms were refined with anisotropic displacement parameters except in **(Ni-TriPhenyl-cdc)** where the atoms of the phenyl rings, t-butyl groups and the located DMF solvent molecule were refined with isotropic parameters to conserve a reasonable data/parameter ratio. All hydrogen atoms were treated as idealized contributions with geometrically calculated positions and with U_{iso} equal to 1.2 U_{eq} (1.5 U_{eq} for methyl) of the attached atom.

Atomic scattering factors are contained in the SHELXTL program library.[2] The structures have been deposited at the Cambridge Structural Database under the following CCDC depositary numbers: CCDC 2181532-2181537.

Table 2. Crystal data and structure refinement details.

Compound	Co-TriPhenyl-cdc	Ni-9-tButylBenzyl-cdc	Ni-TriPhenyl-cdc
Sum Formula	$C_{210}H_{170}Co_8N_4O_{42}S_8$	$C_{190}H_{269}N_{22}Ni_6O_{54}S_8$	$C_{256}H_{276}N_{20}Ni_8O_{58}S_8$
Moiety Formula	$C_{210}H_{170}Co_8N_4O_{42}S_8$, 14[$C_3H_7NO$]	$C_{142}H_{157}N_4Ni_8O_{38}S_8$, 16[$C_3H_7NO$]	$C_{208}H_{164}N_4Ni_8O_{42}S_8$, 2($C_3H_7NO$), 14[$C_3H_7NO$]
Formula Weight, g/mol	4149.14	4334.00	5287.11
Temperature, K	120.0	120.0	150.0
Crystal system	monoclinic	monoclinic	monoclinic
Space group	$P2_1/c$	$C2/c$	$P2_1/c$
Cell dimensions			
a, Å	23.571(3)	46.824(10)	23.513(2)
b, Å	22.245(3)	23.573(5)	22.1099(18)
c, Å	23.653(3)	40.269(9)	24.667(2)
α, °	90	90	90
β, °	101.993(6)	102.204(12)	102.983(4)
γ, °	90	90	90
Volume, $Å^3$	12131(3)	43450(16)	12495.7(18)
Z	2	8	2
ρ_{calc}, g/cm^3	1.136	1.325	1.405
μ/mm^{-1}	5.332	1.948	1.955
F(000)	4276.0	18328.0	5536.0
Reflections collected	60088	95491	59549
Independent reflections	7155	30269	7396
Data/restraints/parameters	7155/2560/1243	30269/3177/1819	7396/1053/793
Goodness-of-fit	1.115	1.052	1.165
R [I>=2σ (I)] R1/wR2	0.1129/0.2567	0.1039/0.3000	0.1711/0.3990
R indexes [all data] R1/wR2	0.1292/0.2667	0.1496/0.3344	0.1862/0.4068
CCDC	2181532	2181533	2181534

Table 2. Crystal data and structure refinement details. (continued)

Compound	Fe-SC4A	Mn-TriPhenyl-cdc	Mg-TriPhenyl-cdc
Sum Formula	$C_{55}FeH_{83}N_3O1_8S_4$	$C_{238}H_{164}Mn_8N_4O_{42}S_8$	$C_{236}H_{236}Mg_8N_{14}O_{50}S_8$
Moiety Formula	$C_{48}H_{64}FeN_2O_{15}S_4$, $1[C_3H_7NO]$, $2[C_2H_6O]$	$C_{208}H_{164}Mn_8N_4O_{42}S_8$, 14 $[C_3H_7NO]$	$C_{208}H_{164}Mg_8N_4O_{42}S_8$, $2(C_2H_8N)$, $4(C_3H_7NO)$, $2[C_3H_7NO]$
Formula Weight, g/mol	1258.33	4087.42	4519.33
Temperature, K	150.0	150.0	150.0
Crystal system	monoclinic	monoclinic	triclinc
Space group	$P2_1/c$	$P2_1/c$	P-1
Cell dimensions			
a, Å	16.457(4)	22.514	13.6310(8)
b, Å	16.110(4)	22.114	19.4305(11)
c, Å	23.679(8)	24.366	22.6660(14)
α, °	90	90	80.495(3)
β, °	98.337(12)	99.54	88.866(3)
γ, °	90	90	76.732(3)
Volume, Å^3	6211(3)	11963.5	5761.8(6)
Z	3	2	1
ρ_{calc} g/cm^3	1.346	1.135	1.302
μ/mm^{-1}	3.791	4.494	1.590
F(000)	2672.0	4208.0	2374.0
Reflections collected	52371	144863	103137
Independent reflections	4556	16571	11619
Data/restraints/parameters	4556/680/509	16571/2241/1060	11619/1026/1179
Goodness-of-fit	1.088	1.057	1.072
R [I>=2σ (I)] R1/wR2	0.1494/0.4642	0.1467/0.3197	0.1115/0.2602
R indexes [all data] R1/wR2	0.1504/0.4707	0.1815/0.3434	0.1186/0.2641
CCDC	2181535	2181536	2181537

References:

1. Apex4 [Computer Software]; Bruker AXS Inc.: Madison, WI, USA, 2021.

2. G.M. Sheldrick, "SHELXT: Integrated space-group and crystal-structure determination". *Acta Cryst.* 2015, ***A71***, 3–8.

3. G. M. Sheldrick, "Crystal structure refinement with SHELXL". *Acta Cryst.* 2015, **C71**, 3–8.

4. A. L. Spek, "Platon Squeeze: a tool for the calculation of the disordered solvent contribution to the calculated structure factors". *Acta Cryst.* 2015, **C71**, 9–18.